

Sequence Dependence of Peptide Fragmentation Efficiency Curves Determined by Electrospray Ionization/Surface-Induced Dissociation Mass Spectrometry

Jennifer L. Jones, Ashok R. Dongré, Árpád Somogyi,[†] and Vicki H. Wysocki*

Department of Chemistry
Virginia Commonwealth University
Richmond, Virginia 23284-2006

Received December 27, 1993

A gas-phase environment allows investigation of "unperturbed", i.e., solvent-free, structures of peptides. Although these structures may not be equivalent to those in the biological environment, the main features, which are controlled by the sequence of the peptide, may be similar in both cases. Tandem mass spectrometry (MS/MS) provides a method for the investigation of peptide structure,^{1a} including peptide conformation,^{1b} in the gas phase. The new MS/MS approach used here combines electrospray ionization (ESI)² with surface-induced dissociation (SID)^{3–6} to determine fragmentation efficiency curves, which are shown to depend on the amino acid sequence of peptides. The curves are obtained by producing the protonated molecules of interest with ESI, colliding the selected MH⁺ ions into a surface, and recording the SID spectra. Fragmentation efficiency curves are a measure of how easily a peptide fragments and are obtained by plotting fragmentation data acquired at a number of different collision energies, with a correction factor for peptide mass [$\Sigma(\text{fragment ion intensity})/\Sigma(\text{total ion intensity})$] vs (collision energy)/(degree of freedom (DOF) ratio⁷). The sequence dependence of these curves can be combined with information on the specific fragment ions formed and with our previous quantum chemical calculations⁵ to predict the relative energy necessary to promote proton transfer and subsequent fragmentation of protonated peptides as a function of sequence.

In Figure 1, fragmentation efficiency curves are illustrated which were chosen to represent peptides with no basic residues, with a basic residue at the carboxy (C) terminus, and with a basic residue at the amino (N) terminus. Hereafter, basic residues will be indicated by the appropriate single letter code in boldface type, e.g., Arg = **R** and Lys = **K**. Figure 1 shows that the absence

[†] On leave from Central Research Institute for Chemistry of the Hungarian Academy of Sciences, P.O. Box 17, H-1525, Budapest, Hungary.

(1) (a) Carr, S. A.; Hemling, M. E.; Bean, M. F.; Roberts, G. D. *Anal. Chem.* **1991**, *63*, 2802–2824. (b) Cheng, X.; Wu, Z.; Fenselau, C. *J. Am. Chem. Soc.* **1993**, *115*, 4844–4848.

(2) (a) Dole, M.; Mack, L. L.; Hines, R. L.; Mobley, R. C.; Ferguson, L. D.; Alice, M. B. *J. Chem. Phys.* **1968**, *49*, 2240–2249. (b) Fenn, J. B.; Mann, M.; Meng, C. K.; Wong, S. F.; Whitehouse, C. M. *Science*, **1989**, *246*, 64–71. (c) Smith, R. D.; Loo, J. A.; Edmonds, C. G.; Barinaga, C. J.; Udseth, H. R. *Anal. Chem.* **1990**, *62*, 882–899.

(3) Cooks, R. G.; Ast, T.; Mabud, Md.A. *Int. J. Mass Spectrom. Ion Processes* **1990**, *100*, 209–265.

(4) The experimental setup used to obtain the required spectra has been described: (a) McCormack, A. L.; Jones, J. L.; Wysocki, V. H. *J. Am. Soc. Mass Spectrom.* **1992**, *3*, 859–862. (b) Wysocki, V. H.; Ding, J.-M.; Jones, J. L.; Callahan, J. H.; King, F. L. *J. Am. Soc. Mass Spectrom.* **1992**, *3*, 27–32.

(5) (a) McCormack, A. L.; Somogyi, Á.; Dongré, A. R.; Wysocki, V. H. *Anal. Chem.* **1993**, *65*, 2859–2872. (b) Somogyi, Á.; Wysocki, V. H.; Mayer, I. *J. Am. Soc. Mass Spectrom.*, in press.

(6) For the details of the preparation of the self-assembled monolayers for SID studies in our laboratory, see: Somogyi, Á.; Kane, T. E.; Ding, J.-M.; Wysocki, V. H. *J. Am. Chem. Soc.* **1993**, *115*, 5275–5283. The chemically-modified surface used in this experiment was a monolayer of octadecanethiolate on gold.

(7) The collision energy was divided by a degree of freedom (DOF) ratio which was obtained by dividing the DOF of a given peptide by the DOF of leucine enkephalin. This calculation assumes that all degrees of vibrational freedom available are active. This may be an overestimation and could lead to decreased differences between curve positions. Without this consideration, the difference between curves is typically 10–15 eV (lab) greater than shown in Figure 1.

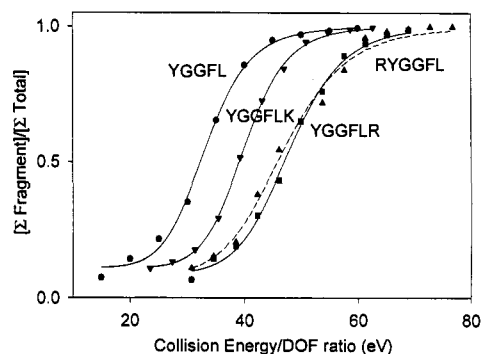


Figure 1. Fragmentation efficiency curves of MH⁺ ions (ESI) for leucine enkephalin, leucine enkephalin-Lys, leucine enkephalin-Arg, and Arg-leucine enkephalin. The y axis represents $\Sigma(\text{fragment ion intensity})/\Sigma(\text{total ion intensity})$, and the x axis represents SID collision energy/DOF ratio normalized to leucine enkephalin.

of a basic residue (YGGFL) results in a population of protonated peptides that fragment more easily at a given collision energy than peptides containing a basic residue (YGGFLK, YGGFLR, and RYGGFL). Also, peptides containing lysine (YGGFLK) have lower energy onsets for fragmentation than those containing arginine (YGGFLR and RYGGFL), which mimics the order of the gas-phase basicities of arginine and lysine.⁸ Shifts similar to those of Figure 1 were observed for other peptides investigated.

For peptides containing a residue with a basic side chain, the high, relatively sharp onset energy for fragmentation is in agreement with the formation of a population of protonated structures containing a dominant, stable protonated form of the peptide.⁹ If the population of ions produced by ESI consists of a large range of different structures with protons located in a way that promotes cleavage, e.g., protonation at an amide nitrogen leading to direct "b" ion formation, then large differences in onset energy would not be expected as a function of amino acid sequence. If fragmentation occurred mainly remote to the site of charge in all cases, the energy required for fragmentation would likewise not depend dramatically on sequence. If, however, a dominant stable structure exists for peptides with a basic residue, high average internal energies from the surface collisions would be required to promote intramolecular proton transfers from this stable form to other less basic sites including the amide nitrogen(s). These transfers initiate fragmentation and are indicated by the types of fragment ions detected, e.g., b and y-type ions whose formation can be rationalized by location of the proton in the vicinity of the cleavage site.⁵ (These conclusions regarding singly-charged ions are in agreement with recent deductions of Gaskell^{9a} and of Boyd^{9b} regarding the presence of mobile protons in doubly-protonated peptides.)

The dominant structure formed by ESI of a peptide with a basic residue could be simply the (basic) side-chain-protonated form or a form containing an intramolecular hydrogen bond between the basic amino side chain (e.g., Arg or Lys) and the amino terminus. In the case of RYGGFL, the arginine side chain can interact (via H-bonding) with the N-terminus to form a stable, cyclic structure. Space-filling models for YGGFLK and YGGFLR show that even in these peptides the side chains of lysine and arginine can interact (via H-bonding) with the N-terminus to form stable, cyclic structures. If proton localization is occurring, modification of the peptide structure should shift the fragmenta-

(8) (a) Gorman, G. S.; Spier, J. P.; Turner, C. A.; Amster, I. J. *J. Am. Chem. Soc.* **1992**, *114*, 3986–3988. (b) Bliznyuk, A. A.; Schaefer, H. F., III; Amster, I. J. *J. Am. Chem. Soc.* **1993**, *115*, 5149–5154.

(9) (a) Bulet, O.; Orkiszewski, R. S.; Ballard, K. D.; Gaskell, S. J. *Rapid Commun. Mass Spectrom.* **1992**, *6*, 658–662. (b) Tang, X.-J.; Thibault, P.; Boyd, R. K. *Anal. Chem.* **1993**, *65*, 2824–2834. (c) Johnson, R. S.; Martin, S. A.; Biemann, K. *Int. J. Mass Spectrom. Ion Processes* **1988**, *86*, 137–154. (d) Poulter, L.; Taylor, L. C. E. *Int. J. Mass Spectrom. Ion Processes* **1989**, *91*, 183–197.

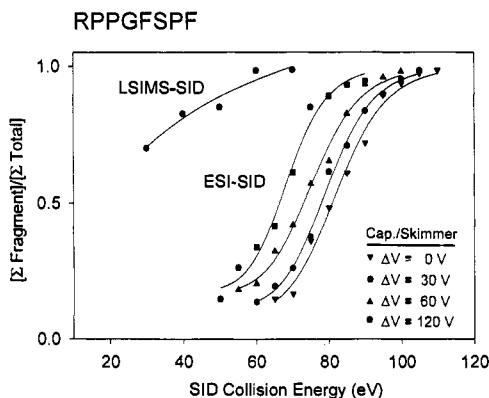


Figure 2. Fragmentation efficiency curves of MH^+ ions for des- R^9 -bradykinin formed by ESI and LSIMS. For ESI/SID, the curves represent four different capillary-skimmer voltage differences (ΔV). The y axis represents $\Sigma(\text{fragment ion intensity})/\Sigma(\text{total ion intensity})$, and the x axis represents SID collision energy.

tion efficiency curve in a predictable manner. ESI/SID of the diacetylation product of the N-terminal Arg of des- R^9 -bradykinin (RPPGFSPF), for example, leads to a lower onset energy for fragmentation (data not shown) than that for des- R^9 -bradykinin. This result is consistent with a decrease in basicity and/or removal of possible H-bonding sites upon acetylation.

If the above arguments regarding formation of a stable dominant structure are correct, the fragmentation efficiencies determined by ESI/SID should show a strong dependence on the ion preparation conditions. Figure 2 illustrates that this is the case by showing the influence of the ionization method on fragmentation efficiency curves (Cs^+ ion bombardment labeled as LSIMS-SID; ESI-SID at various capillary-skimmer voltage differences (ΔV)). For ESI/SID, the fragmentation efficiency curves can be shifted by changing the potential difference (ΔV) between the capillary and skimmer of the ESI source or, less easily, by changing the temperature of the capillary. As ΔV is increased, the precursor ion is collisionally activated (i.e., "heated up") prior to collision with the surface and thus the SID collision energy required for a given extent of fragmentation is decreased. Figure 2 also indicates that the MH^+ ions formed by ESI are more difficult to fragment than MH^+ ions produced by 6 keV Cs^+ ion bombardment. This significant shift of the LSIMS/SID curve to lower SID collision energies in Figure 2 is in agreement with other researchers' comments that ions produced by ESI are more difficult to fragment than those formed by LSIMS. Our interpretation of this effect (which was also recorded for the other compounds discussed above) includes two interchangeable contributing factors: (i) MH^+ ions formed by ESI are internally

colder than those produced by LSIMS, and (ii) the relative populations of various possible protonated forms are different for the two ionization methods, with fewer distinct protonated forms of a single peptide produced by ESI than by LSIMS.¹⁰ Because increased internal energy can lead to interconversion of various protonated forms, it is not possible to unequivocally state that one of the above factors is a greater contributor than the other.

Note that all curves shown in Figure 1 were obtained at $\Delta V = 30$ V. Under these conditions, even the most fragile peptide investigated here, YGGFL, shows no gas-phase collision-induced fragmentation in the capillary-skimmer region. Use of a consistent set of experimental conditions assures that the relative energetics of dissociation reflect structural features of the compounds of interest. As discussed above, the relatively steep slopes of the ESI/SID curves obtained at $\Delta V = 30$ V show dramatic changes in the extent of peptide fragmentation as a function of ion-surface collision energy (Figure 1). This suggests that (i) the distribution of energies deposited into peptides by surface collisions is narrow, in agreement with the narrow distributions established in numerous studies of small ions, and (ii) the distribution of energy deposited by ESI is narrow.^{3,4b} As the distribution of energies deposited by the ionization method is broadened, e.g., by using Cs^+ ion bombardment, the slope of the fragmentation efficiency curve decreases.

Our data show that protonated peptides formed by ESI are more difficult to fragment than peptides produced by 6 keV Cs^+ ion bombardment. Relative onset energies from ESI/SID fragmentation efficiency curves depend strongly on the amino acid sequence of gas-phase protonated peptides. The sharp onset energies of the fragmentation efficiency curves suggest that the population of ion structures formed by ESI is not as complex as that formed by LSIMS and that a stable dominant form exists for peptides with a basic amino acid. Further systematic development of this approach to include synthetic peptides designed to contain or not contain potential hydrogen-bonding sites could increase our knowledge of intramolecular hydrogen bonding, especially if the technique proves to be sensitive to differences in conformations (*secondary structures*) of peptides. Further application of this method will also improve our basic knowledge of how protonated peptides and other large molecules fragment and could lead to improved rules for automated interpretation programs for peptide sequencing.

Acknowledgment. This work was supported by a grant from NSF (CHE-9224719).

(10) The shift of the LSIMS/SID fragmentation efficiency curve relative to the ESI/SID fragmentation efficiency curves (Figure 2) is too large to be explained by the small measured differences in the kinetic energy distributions associated with the two ionization methods.